



Published in final edited form as:

Nat Neurosci. 2008 April ; 11(4): 420–422. doi:10.1038/nn2073.

ALS-causing SOD1 mutants generate vascular changes prior to motor neuron degeneration

Zhihui Zhong¹, Rashid Deane¹, Zarina Ali¹, Margaret Parisi¹, Yuriy Shapovalov², Kerry O'Banion², Konstantin Stojanovic¹, Abhay Sagare¹, Severine Boillee³, Don W. Cleveland³, and Berislav V. Zlokovic¹

¹ Center for Neurodegenerative and Vascular Brain Disorders and Departments of Neurosurgery and Neurology, University of Rochester Medical Center, Rochester, NY

² Department of Neurobiology and Anatomy, University of Rochester Medical Center, Rochester, NY

³ Ludwig Institute and Departments of Medicine and Neuroscience, University of California at San Diego, La Jolla, CA

Abstract

We report ALS-linked superoxide dismutase-1 (SOD1) mutants of different biochemical characteristics disrupt the blood-spinal cord barrier in mice by reducing the levels of the tight junction proteins ZO-1, occludin and claudin-5 between endothelial cells. This results in microhemorrhages with release of neurotoxic hemoglobin-derived products, reductions in microcirculation and hypoperfusion. SOD1-mutant mediated endothelial damage accumulates prior to motor neuron degeneration and neurovascular inflammatory response, supporting a central contribution to disease initiation.

The current model of disease mechanism caused by amyotrophic lateral sclerosis (ALS)-linked superoxide dismutase-1 (SOD1) mutations is that toxicity derived from non-neuronal neighboring cells, particularly microglia and astrocytes, contributes to motor neuron degeneration and disease progression^{1,2}. The role of blood vessels in the pathogenesis of ALS, however, is poorly understood. A recent report documented ultrastructural changes at the blood-spinal cord barrier (BSCB)³, as well as BSCB leakage to Evans blue⁴, midway through disease progression in a disease model generated by transgenic overexpression of a dismutase active ALS linked SOD1 mutant (SOD1^{G93A}). Whether damage to the vasculature is a feature common to dismutase active and inactive SOD1 mutants causative of ALS, and whether it affects microcirculation within the spinal cord are all unknown. We now use mouse models that express SOD1 mutants of different biochemical characteristics to address these questions.

Address Correspondence: Berislav V. Zlokovic, Arthur Kornberg Medical Research Bldg., 601 Elmwood Ave., Box 645, Rochester, New York 14642, Tel: 585-273-3132; Fax: 585-273-3133, Berislav_Zlokovic@urmc.rochester.edu.

AUTHOR CONTRIBUTIONS

Z.Z. conducted and performed most of experimental studies, and co-designed some blood-spinal cord barrier permeability studies with B.V.Z. R.D. supervised the regional blood flow studies and analyzed the data. Z.A. conducted TEM study. M.P. performed blood flow studies. Y.S. and K.O. conducted and performed immunostaining and RT-PCR studies for Icam-1 and Cox-2. K.S. performed several immunostaining studies. A.S. performed autoradiography. S.B. and D.W.C. provided essential experimental tools (SOD1^{G37R}, SOD1^{G85R} and SOD1^{WT} mice) and expertise regarding various mouse models that express SOD1 mutants of different biochemical characteristics. D.W.C. provided critical input to the manuscript. B.V.Z. designed the entire study, supervised all portions of the study, and wrote the manuscript.

The BSCB to serum proteins appeared to be nearly intact in the lumbar cord of control mice as indicated by negligible immunoglobulin G (IgG) staining in parenchyma (Fig. 1a–b). In contrast, substantial focal IgG deposits from blood vessels were seen in the lumbar cords of SOD1^{G37R} and SOD1^{G85R} mice at 3.5 and 6.5 months of age, respectively. The intensity of IgG leakage in SOD1^{G37R}, SOD1^{G85R} and SOD1^{G93A} mutants indicated a substantial BSCB breakdown to serum proteins that in each line was prior to or contemporaneous with initial axonal withdrawal from neuromuscular junctions^{5,6}, and prior to motor neuron loss (Fig. 1c). In each line, further increase in IgG leakage was seen during disease progression. Notably, mice over-expressing human wild type SOD1 (SOD1^{WT})⁷ (to levels at or well above the levels of mutant SOD1 in each of the ALS lines) did not develop changes in BSCB permeability to IgG (assayed at 4 and 7 months of age) compared to wild type littermate controls.

Prussian blue staining from presymptomatic SOD1^{G93A}, SOD1^{G37R} and SOD1^{G85R} mice identified deposits of hemosiderin, a hemoglobin derivative, within motor neurons and outside motor neurons (Fig. 1d), suggesting microhemorrhages. All studied SOD1 mutants exhibited significant hemosiderin accumulations presymptotically (Fig. 1e), well prior to motor neuron loss. Hemosiderin deposition worsened with disease progression, but was absent in age-matched C57BL6 and B6SJL littermate controls and mice expressing SOD1^{WT} (Fig. 1d–e). Deposits were found mainly in the anterior horn (Supplementary Fig. 1).

To address whether inflammatory vascular changes take place before BSCB disruption, accumulation of the monocyte chemoattractant protein-1 (MCP-1) and cyclooxygenase-2 (Cox-2), two inflammatory markers mediating blood-brain barrier opening⁸, and Icam-1 (intercellular adhesion molecule-1), a marker of activated endothelium⁹, were studied in SOD1^{G93A} mutants. At 2 months of age, when the BSCB is already disrupted in SOD1^{G93A} mice (Fig. 1a–b, d–e), there was no an increase in *MCP-1* (Fig. 1f), *Cox-2* or *Icam-1* mRNA levels (Fig. 1g–h), and/or immunostaining (Supplementary Figs. 2 and 3). In contrast, these markers were elevated at 3.5 months. Our findings are consistent with prior observations in human SOD1^{G93A} mutants, showing no microglia activation at 2 months¹⁰ (confirmed in our study; not shown), an increased MCP-1 expression at the symptomatic and end stages, but not at an early stage^{9,10}, and increased mRNA levels for numerous potential mediators involved in microglia propagation at symptomatic and end stages, but not at an early presymptomatic stage^{1,9}. Thus, the BSCB breakdown observed at an early pre-symptomatic stage in SOD1^{G93A} mutants precedes the neurovascular inflammatory response. At later stages, however, activation of different inflammatory markers likely contributes to the observed progressive BSCB breakdown (Fig. 1b; Fig 1e).

An early BSCB breakdown prior to inflammatory changes could be a consequence of SOD1 direct toxicity to the endothelium and disruption of tight-junction integrity. To test this, immunoblotting of extracts of isolated spinal cord capillaries, a site of the BSCB *in vivo*, was used to measure levels of proteins that are essential for the formation of the barrier compared with proteins that do not participate in the barrier formation. As expected, human SOD1 mutant was expressed in endothelium in SOD1^{G93A} mice (Fig. 2a). Mouse endogenous SOD1 expression was not altered by SOD1^{G93A} mutation. In contrast, in 2 month old SOD1^{G93A} mice, the levels of ZO-1, occludin and claudin-5 (Fig. 2a), the tight junction proteins which mediate low paracellular permeability between adjacent endothelial cells⁸, were reduced by 40–60%. Accumulation of other endothelial antigens that are not involved in the formation of the barrier, e.g., the glucose transporter Glut1 and von Willebrand factor (not shown)⁸, were not affected by SOD1 mutation (Fig. 2a). Immunoblot analysis of spinal cord capillaries derived from mice expressing ALS-linked SOD1 mutants that retain full (SOD1^{G37R}) or no (SOD1^{G85R}) dismutase activity, but not

SOD1^{WT}, revealed similar downregulation of the tight junction proteins in endothelium (Fig. 2b), at ages prior to initiation of motor neuron degeneration (3.5 and 6.5 months, respectively⁶). Immunostaining for ZO-1 in the vasculature corroborated 40–50% reductions in SOD1^{G37R} and SOD1^{G85R} mice (Supplementary Fig. 4). These data suggest that SOD1-mutant toxicity specifically disrupts the BSCB by reducing accumulation of critical tight junction proteins in the endothelium.

Significant ($P < 0.01$) 10–15% reductions in the total length of capillaries in the lumbar cord of SOD1^{G93A}, SOD1^{G37R} and SOD1^{G85R} mice were found compared to wild type littermate controls or SOD1^{WT} mice (Fig. 2c) at stages prior to motor neuron loss (Fig. 1c)^{5,6} and prior to inflammatory changes (Fig. 1f–g). Electron microscopy of SOD1^{G37R}, SOD1^{G85R} mice or SOD1^{G93A} mutant mice at ages prior to denervation (3.5, 6 and 2 months, respectively) revealed focal accumulations of extracellular fluid (edema) between the capillary vessel wall and motor neurons, and/or collapsed capillary lumens in all three models (Fig. 2d). In contrast, littermate controls showed a normal vascular-neuronal relationship (Fig. 2e).

We next tested if the BSCB breakdown and reductions in total capillary length and microhemorrhages affected blood flow. Direct measurement (with ¹⁴C-iodoantpyrine) revealed 30% to 45% reductions through the cervical and lumbar cord, respectively, by 2 months of age in SOD1^{G93A} mice (Fig. 2f). Early reductions in the blood flow were most prominent in the anterior horn in the lumbar cord, the region most affected in each of the mouse models (Supplementary Fig. 5). Reductions in flow would be expected to create chronic hypoperfusion, which could aggravate motor neuron injury and functional outcome, as shown in mice with a mutation that eliminates hypoxia-responsive induction of the vascular endothelial growth factor (*Vegf*) gene (*Vegfa*^{δδ}) and which develop late-onset motor neuron degeneration¹¹. Ischemia worsened motor neuron degeneration and functional outcome in *Vegfa*^{δδ} mice, whereas the absence of hypoxic induction of VEGF in mice that develop motor neuron disease from expression of ALS-linked mutant SOD1^{G93A} yield substantially reduced survival¹².

Free hemoglobin released from extravasated red blood cells confers direct toxicity to neurons¹³ by releasing neurotoxic products (e.g., free iron) associated with generation of reactive oxygen species (ROS), lipid peroxidation and neuronal cell death. Consistent with hemoglobin-mediated damage reported in other contexts¹³, SOD1^{G37R} and SOD1^{G85R} mutations, but not SOD1^{WT}, increased significantly ($P < 0.05$) susceptibility of N2a neuronal cells¹⁴ to hemoglobin-mediated cell death (Fig. 2g).

More recent studies reported an increase in the CSF/serum albumin ratio in a subset (< 30%) of sporadic ALS patients¹⁵, but spinal cord tissue and BSCB have not been analyzed directly. The present study demonstrates that changes to the vasculature seem likely to contribute in an important way to degeneration of large motor neurons in familial models of ALS. Moreover, we have shown that damage to the vasculature is one of the earliest pathologic events in the toxic cascade from both dismutase active and inactive SOD1 mutants including a disruption of the BSCB mediated by reduced levels in the endothelium of the essential tight-junction proteins ZO-1, occludin and claudin-5, resulting in microhemorrhages that release neurotoxic products, reductions in microcirculation and hypoperfusion (Supplementary Fig. 6). All of this evidence supports a central contribution of mutant mediated damage to the vasculature in initiating non-cell autonomous killing of motor neurons in inherited ALS. Genetic or pharmacologic interventions targeted specifically at the endothelium are now warranted to determine the causality between BSCB leakage and motor neuron degeneration and how such damage may delay disease onset and/or its progression.

For detailed Methods see Supplemental information.

Supplementary Material

Refer to Web version on PubMed Central for supplementary material.

Acknowledgments

This work was supported by the United States National Institutes of Health grants R37 AG023084, R37 NS34467 and HL63290 to BVZ and R37 NS27036 to DWC and a Muscular Dystrophy Association grant to MKO. SB is supported by a development grant from the Muscular Dystrophy Association. We thank Karen L. Bentley, Director of the EM Research Core at the University of Rochester for skillful processing of EM samples.

References

1. Boillée S, Vande Velde C, Cleveland DW. ALS: a disease of motor neurons and their nonneuronal neighbors. *Neuron* 2006;52:39–59. [PubMed: 17015226]
2. Boillée S, et al. Onset and progression in inherited ALS determined by motor neurons and microglia. *Science* 2006;312:1389–1392. [PubMed: 16741123]
3. Garbuzova-Davis S, et al. Ultrastructure of blood-brain barrier and blood-spinal cord barrier in SOD1 mice modeling ALS. *Brain Res* 2007;1157:126–137. [PubMed: 17512910]
4. Garbuzova-Davis S, et al. Evidence of compromised blood-spinal cord barrier in early and late symptomatic SOD1 mice modeling ALS. *PLoS ONE* 2007;2:e1205. [PubMed: 18030339]
5. Pun S, et al. Selective vulnerability and pruning of phasic motoneuron axons in motoneuron disease alleviated by CNTF. *Nat Neurosci* 2006;9:408–419. [PubMed: 16474388]
6. Lobsiger C, et al. Toxicity from different SOD1 mutants dysregulates the complement system and the neuronal regenerative response in ALS motor neurons. *Proc Natl Acad Sci USA* 2007;104:7319–7326. [PubMed: 17463094]
7. Gurney ME, et al. Motor neuron degeneration in mice that express a human Cu,Zn superoxide dismutase mutation. *Science* 1994;264:1772–1775. [PubMed: 8209258]
8. Zlokovic BV. Neurovascular mechanisms of Alzheimer's neurodegeneration. *Trends Neurosci* 2005;28:202–208. [PubMed: 15808355]
9. Sargsyan S, Monk PN, Shaw PJ. Microglia as potential contributors to motor neuron injury in amyotrophic lateral sclerosis. *GLIA* 2005;51:241–253. [PubMed: 15846792]
10. Hall E, Oostveen JA, Gurney ME. Relationship of microglial and astrocytic activation to disease onset and progression in a transgenic model of familial ALS. *GLIA* 1998;23:249–256. [PubMed: 9633809]
11. Oosthuysen B, et al. Deletion of the hypoxia-response element in the vascular endothelial growth factor promoter causes motor neuron degeneration. *Nat Genet* 2001;28:131–138. [PubMed: 11381259]
12. Lambrechts D, et al. VEGF is a modifier of amyotrophic lateral sclerosis in mice and humans and protects motoneurons against ischemic death. *Nat Genet* 2003;34:383–394. [PubMed: 12847526]
13. Regan RF, Guo Y. Toxic effect of hemoglobin on spinal cord neurons in culture. *J Neurotrauma* 1998;15:645–653. [PubMed: 9726263]
14. Pasinelli P, Borchelt DR, Houseweart MK, Cleveland DW, Brown RH Jr. Caspase-1 is activated in neural cells and tissue with amyotrophic lateral sclerosis-associated mutations in copper-zinc superoxide dismutase. *Proc Natl Acad Sci USA* 1998;95:15763–15768. [PubMed: 9861044]
15. Brettschneider J, Petzold A, Süßmuth SD, Ludolph AC, Tumani H. Axonal damage markers in cerebrospinal fluid are increased in ALS. *Neurol* 2006;66:852–856.

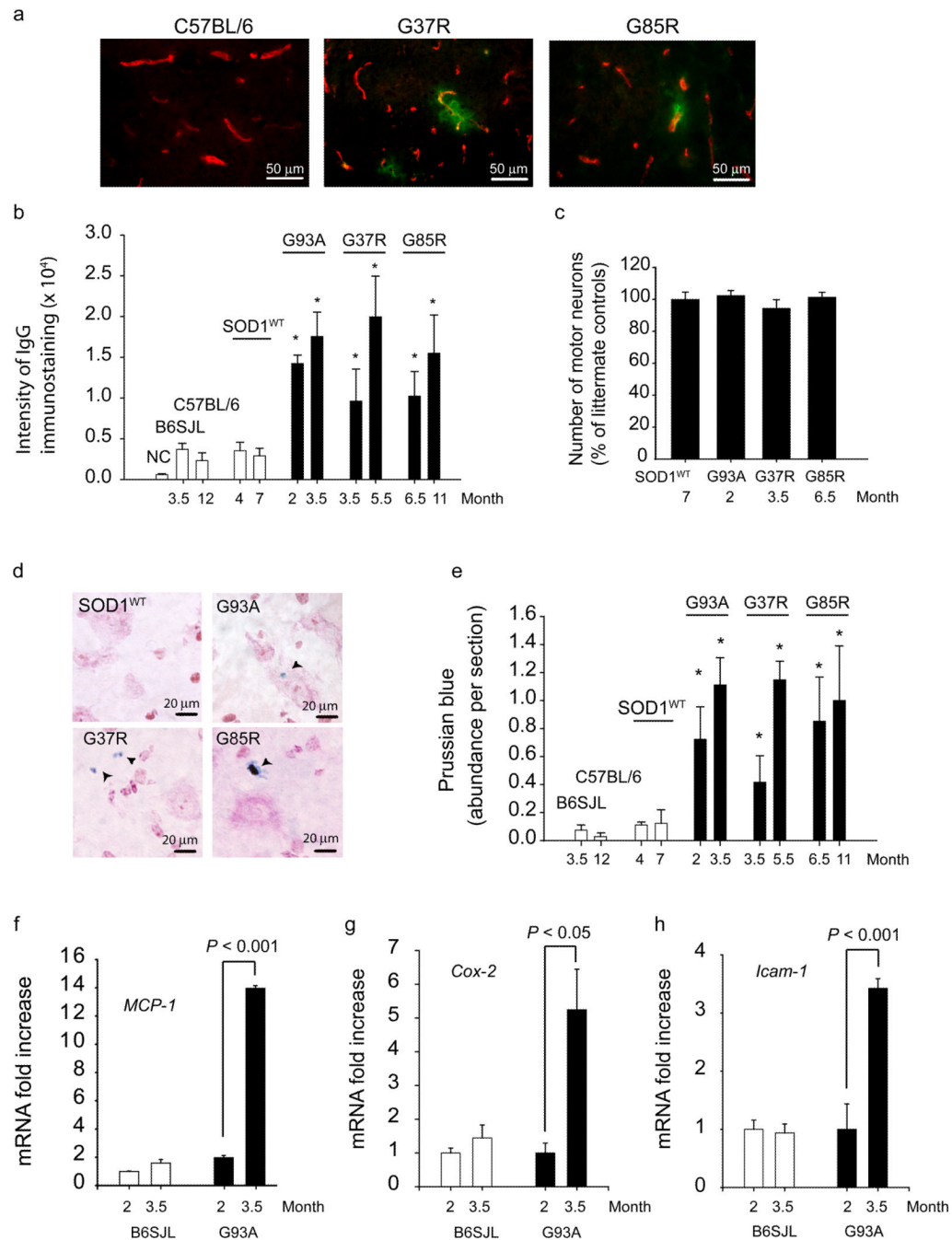


Figure 1. Breakdown of the blood-spinal cord barrier with microhemorrhages in different SOD1 mutants presymptomatically

(a) Double immunostaining for IgG (green) and CNS endothelium (CD31, red) in the lumbar spinal cord of wild type mouse and 3.5 months old SOD1^{G37R} and 6.5 months old SOD1^{G85R} mutants. (b) Quantification of the IgG signal intensity in the lumbar spinal cord of different SOD1 mutants at varying ages compared to their respective controls and SOD1^{WT} mice. NC, negative controls (omission of IgG antibody). (c) The number of motor neurons in the lumbar cord of different SOD1 mutants at an early stage of the disease process and in SOD1^{WT} mice expressed as a percentage of total number of motor neurons in non-transgenic controls. (d) Hemosiderin extra-neuronal and neuronal deposition in the

lumbar spinal cords in different SOD1 mutants, but not in SOD1^{WT} mice. **(e)** Quantification of hemosiderin deposits in the lumbar spinal cord of different SOD1 mutants, controls and SOD1^{WT} mice. **(f–h)** Quantitative RT-PCR analysis of mRNA transcripts for *MCP-1*, *Cox-2* and *Icam-1* in the lumbar spinal cord of SOD1^{G93A} mice and controls at different age. Values are means \pm s.e.m., n = 3–6 mice per group. **P* < 0.05 compared to SOD1^{WT} or non-transgenic mice. All procedures were according to the NIH guidelines and approved by the University of Rochester Committee on Animal Resources.

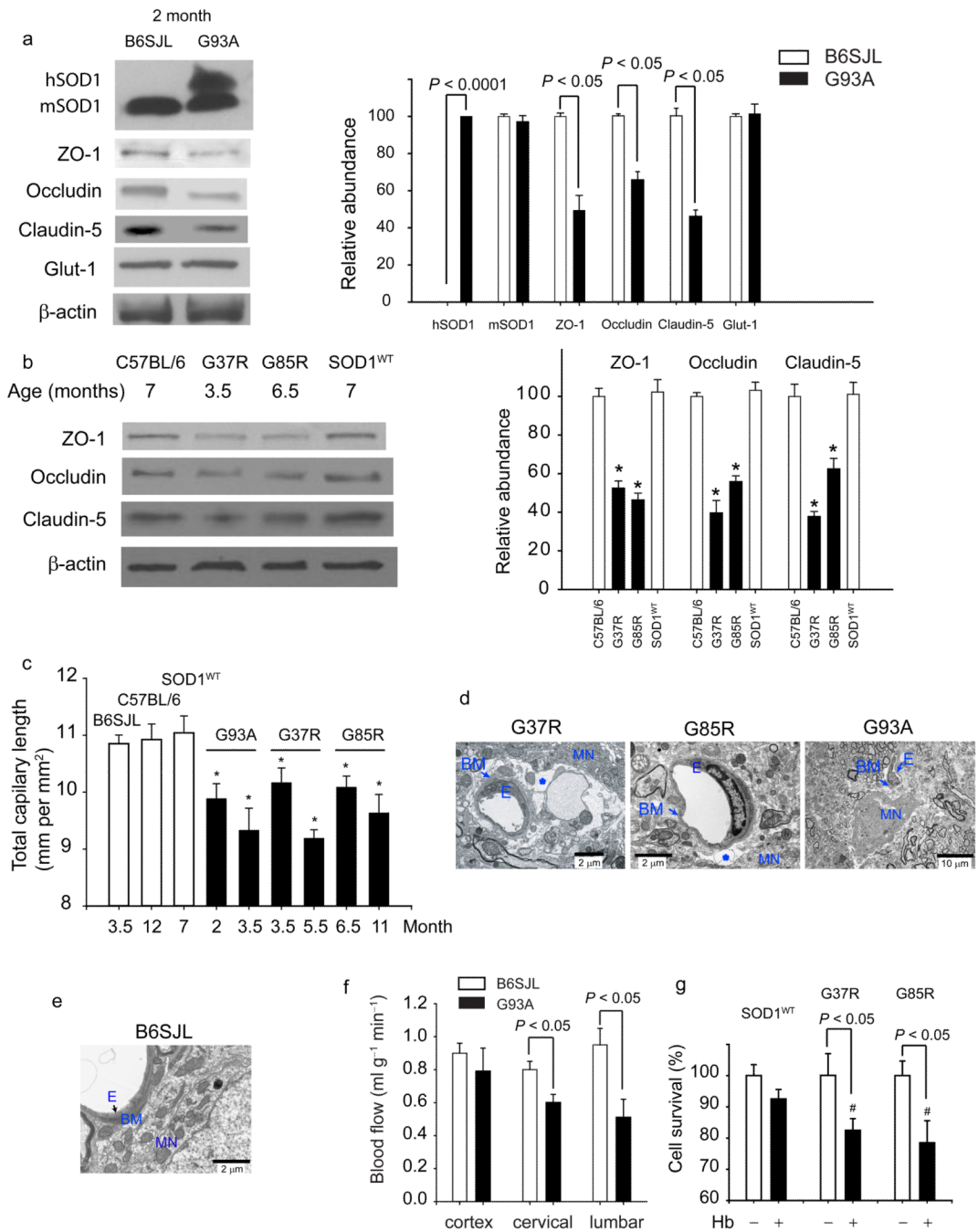


Figure 2. SOD1 toxicity to endothelium results in loss of tight junction proteins and reductions in microcirculation and blood flow

(a) Immunoblot analysis of human hSOD1, mouse mSOD1, ZO-1, occludin and claudin-5, and Glut-1 in spinal cord microvessels from 2 months old SOD1^{G93A} mice compared to controls. Graph - band density for test-proteins relative to β-actin. (b) Immunoblot analysis of ZO-1, occludin and claudin-5 in the spinal cord capillaries from 7, 3.5 and 6.5 months old C57BL/6, mice, SOD1^{G37R} and SOD1^{G85R} mutants, respectively, and 7 months old SOD1^{WT} mice. Graph - band density for test-proteins relative to β-actin. **P* < 0.05, SOD1 mutants vs. controls or SOD1^{WT} mice. (c) Total capillary length in the anterior horn of the lumbar spinal cord in SOD1 mutants (mm CD31-positive structures per mm²). **P* < 0.05,

SOD1 mutants vs. age matched controls. **(d–e)** Transmission electron microscopy (TEM) in 3.5 and 6.5 months old SOD1^{G37R} and SOD1^{G85R} mutants, respectively, shows edema (asterisk) between the capillary wall and motor neurons. Collapsed capillary lumen in SOD1^{G93A} mice. E, endothelium; BM, basement membrane, MN, motor neuron. **(e)** TEM of B6SJL mouse shows normal neuronal-vascular contact and intact endothelium. **(f)** Blood flow through the spinal cord and frontal cortex in 8 weeks old SOD1^{G93A} mice compared to controls. **(g)** Hemoglobin (Hb) toxicity to N2a cells transduced with SOD1^{G37R} and SOD1^{G85R} mutants and SOD1^{WT}. #*P* < 0.05, SOD1^{G37R} or SOD1^{G85R} vs. SOD1^{WT}. Mean ± s.e.m. a–c and f, n = 3–5 mice per group. g, n = 4 experiments per group.